The Heidelberg Heavy Ion Cooler Storage Ring T S R [§]

G. Bisoffi, M. Blum, A. Friedrich, C. Geyer, M. Grieser, B. Holzer, H.W. Heyng, D. Habs, E. Jaeschke, A. Jason[+], M. Jung, D. Krämer, K. Matl, A. Noda[×], W.Ott, R.Repnow, F. Schmitt, M. Steck, E. Steffens

Max Planck Institut für Kernphysik Heidelberg
D-6900 Heidelberg, FRG

[+] Los Alamos National Laboratory, Los Alamos

[×] Institute for Nuclear Studies, Tokyo

Summary

Commissioning of the Heidelberg Test Storage Ring TSR started in May 1988. The TSR is a low energy cooler storage ring for heavy ions with energies up to 30 MeV/amu at a charge to mass ratio q/A = 0.5. Phase space cooling for coasting beams as well as for bunched beams is routinely done by electron cooling.

As the ring is fed by a Tandem Linac combination stored intensities of up to 1×10^{10} particles are obtained by combined stacking into transversal and longitudinal phase space (multiturn injection and rf stacking). This stacking method gives 800 times the number of stored ions compared to single turn injection.

Cooling oxygen and carbon beams resulted in a typical emittance of 0.3 π mm mrad and a momentum spread of $\Delta p/p=10^{-4}$. The equilibrium mainly being determined by intrabeam scattering and the heating in the residual gas by multiple scattering. An overall increase of phase space density by 6 orders of magnitudes was observed, similar to cooling results at proton machines [1 - 3]. Results on the first year of operation with heavy ions at TSR are reported.

[§] Funded by BMFT under contract No.: 06 HD 852 I

Introduction

The Heidelberg Heavy Ion Test Storage Ring TSR is a 55.4 m circumferene low energy cooler ring with four fold symmetry, see fig. 1. Eight 45 degree C-shaped dipole magnets accomplish deflection. Always two dipoles with a focussing quadrupole inbetween form the center of one focussing period of the separated function lattice. The focussing periods are completed on both sides by quadrupole dublets and half the long straight sections. Normal optics uses a mode where two antisymmetric focussing periods form one of the two superperiods [4] . The dispersion function D is chosen such that in the injection straight and subsequently in the opposite straight section D = 2 m.

At the end of the transfer line from the injector two magnetic septa and an electrostatic septum inflector are guiding the beam parallel to the ring axis; these injection elements are to be seen in the foreground of fig. 1. As the incoming beam is entering the TSR with a lateral offset of 100 mm parallel to the central orbit, four small dipole magnets create a DC bump of 60 mm amplitude at the electrostatic septum. For multiturn injection four fast bumper magnets are producing a time dependent closed orbit distortion to fill the horizontal acceptance of the ring. A small ferrit loaded cavity is installed for adiabatic capture of the beam. The particles in the buckets are then decelerated by a constant amount in momentum. Successive repetition of this 'stacking to the top' allows accumulation of many multiturn batches enlarging the number of stored ions by nearly 3 orders of magnitude compared to single turn injection resulting in 10^{10} stored particles as envisaged.

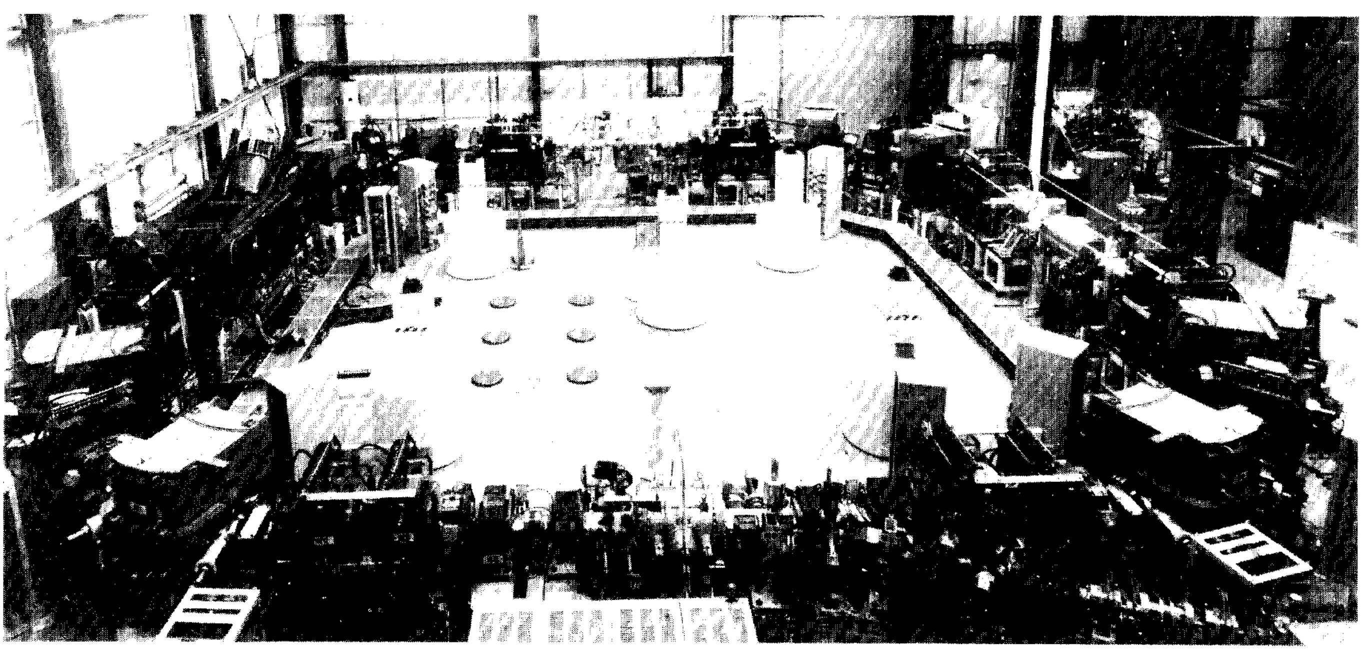

Fig. 1 The Heidelberg Test Storage Ring for Heavy Ions TSR, the Electron cooler is situated in the straight section at left.

CH2669-0/89/0000-0049$01.00©1989 IEEE

Commissioning of the storage ring started mid of 1988 when a 73 MeV C^{6+} beam was successfully stored [4] . The installation of the Eletron cooler in late 1988 led to a variety of interesting results. Phase space compression of up to a factor of 100 for the transversal planes each as well as a shrinking of momentum spread by two orders of magnitude increased the phase space density by a factor of 10^6 giving beams of emittancies of 0.3 π mm mrad and momentum spread of $\Delta p/p = 10^{-4}$. These values reflected the equilibrium of phase space blow up by multiple scattering in the residual gas and intra beam scattering counteracted by the cooling. As a consequence dramatic increase of beam life time was measured for bare ions.

At intensities of a few pµA collective density fluctuations were seen in the splitting of the Schottky spectrum of coasting beams, as expected for sufficiently cold beams [5].

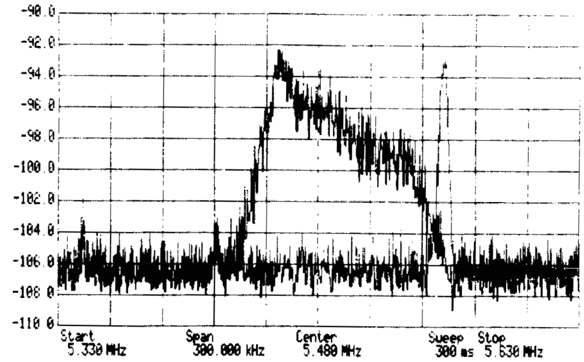

Fig 3. Schottky noise spectrum of a rf stacked C-beam (wide distribution) ; the spectrum of a single multiturn batch is displayed for comparison.

Particle Stacking in the TSR

For injector into TSR the existing 12 MV MP Tandem Postaccelerator Combination [6] at MPI is used. This flexible injector provides a great variety of ion species ranging from proton to lead beams. Energies are up to 5 MeV/amu for the heavier ions and up to 16 MeV/amu for the lighter projectiles. As this injector needs negative ions to start with, the resulting intensities from normal sputter ion sources are relatively small (µA-range). As C-beams at 73 MeV (rigidity of Bρ = 0.71 Tm) is a typical beam at TSR, this beam is taken as an example for the following discussion of particle stacking. By operating the ion source [7] in a pulsed mode it is possible to obtain macro pulses of up to 7×10^{10} negative ions, the pulse width is about 150 µs. These ions being accelerated and stripped in the tandem. At injection into the ring about 10^9 C^{6+} ions per pulse are available. The beam emittance is 1.5 π mm mrad, the momentum spread in the order of 2×10^{-4}. As the acceptance of the ring is rather large (A > 120 π mm mrad, momentum acceptance > +/- 3%) at most 44 turns can be stored as simulations of multiturn injection have shown. After proper setting of the injection parameters storing of 40 turn was measured, giving up to 600 el.µA circulating C^{6+} ions. The 4 bump magnets are generating a field ramp of dB/dt = 100 T/m for a time of 150 revolutions e.g. 120 µs. Metallic vacuum chambers from 0.3 mm thin Inconel 600 are used in the fast bumpers.

Multiturn injected particles are captured adiabatically into a bucket and decelerated by about 2% in momentum, keeping the bucket area constant. The rf frequency is reduced from 6.79 MHz (harmonic number h = 11) by 120 kHz in 14 ms. Fig. 2 shows the rf amplitude (upper trace) and the frequency shift (lower trace) for a complete rf staking cycle. The maximum voltage at the cavity is 400 V. Due to the finite dispersion at the injection point clearance for a new multiturn batch is generated. By sucessive repetition of the stacking cycle (stacking to the top) the equivalent of 18 complete multiturn batches of 380 µA each can be accumulated, giving a total current of 7 mA. These are 1.2×10^{10} stored particles well above the design aim. Fig. 3 displays a Schottky noise spectrum of a rf stacked C^{6+} beam of 73 MeV. The wide distribution reflects a momentum spread of 2% after stacking, the sharp line at the high momentum end of the spectrum is the corresponding multiturn injected beam. The spectra were taken at the 10 th harmonic of the revolution frequency. To compensate for chromatic effects two sextupole families were used to set chromaticites to Q'_x = -0.09 and Q'_y = 0.50. Particle accumulation rates are shown in fig. 4 where the increase in intensity versus the number of multiturn batches added to the stored intensity is plotted. After a steep increase in current which reflects small losses during the first 14 stacks the efficiency of stacking levels off. An equilibrium of losses and gain is reached after 25 stackings, the integrated intensity multiplication factor of rf stacking is 18.

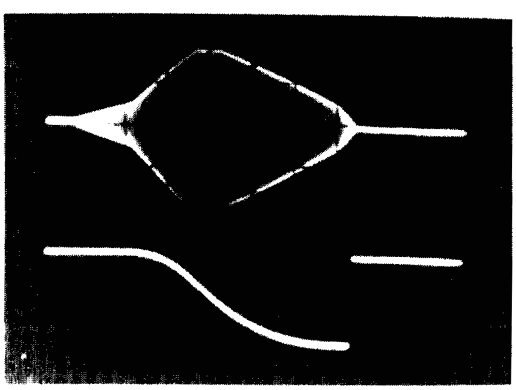

Fig. 2 Rf amplitude (upper trace) and frequency shift (lower trace) of the cavity during a complete stacking cycle.

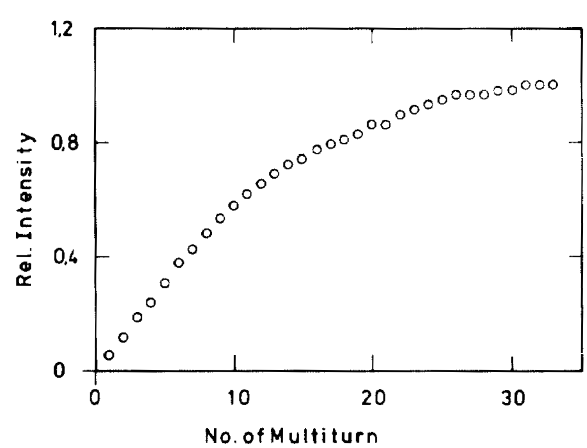

Fig. 4 Intensity increase during rf stacking as function of the number of multiturn batches.

Electron Cooling of Heavy Ions at the TSR

For phase space compression of particle beams an electron cooling device is used at TSR. Fig. 5 shows the cross section of the cooler. The high perveance gun (P = 1.66 μPerv) generates for the 73 MeV C beam setting 0.35 A at an energy of 3.5 keV electrons. The electron beam is guided by a solenoidal field and bent by a dipole field inside the toroid magnet onto the ion beam axis. In the 1.5 m interaction region the electrons travel with the same mean velocity as the circulating ions. The electrons are bent out the beam and finally dumped in a highly efficient collector.

Strong attention was paid to match the solenoids of different diameters as well as the toroids to minimize heating of the electron beam at the junctions. Inside the interaction section the main cooling solenoid's relative transversal field components were reduced to $B_t/B_o < +/- 2\times10^{-5}$ by means of correction coils.

Reduction of momentum spread of a 1.8 mA coasting beam is illustrated in fig. 7. The Schottky spectrum shows the initial momentum distribution of $\Delta p/p = 0.018$ as generated by rf stacking. Within 3 s the beam is cooled to $\Delta p/p = 2\times10^{-4}$ as the peaked momentum distribution indicates. The intensities during cooling remained constant whereas the integrated momentum distribution showed signal depression changing from the wellknown $N^{1/2}$ scaling to the more complex behaviour due to collective phenomena. Expanding the Schottky spectra for the cooled beam, fig. 8, a double peak structure becomes visual as long as the beam intensities exceed a level of a few μA. This splitting is due to counter rotating plasma waves in the beam, as theoretically described in ref. [5] similar to longitudinal phonons in a solid. At small beam intensities this structure of the Schottky spectrum is converted into a Gaussian. For beam intensities of $< 10^7$ particles where intra beam scattering is small, the equilibrium momentum spread of the beam was measured to be a few times 10^{-5}.

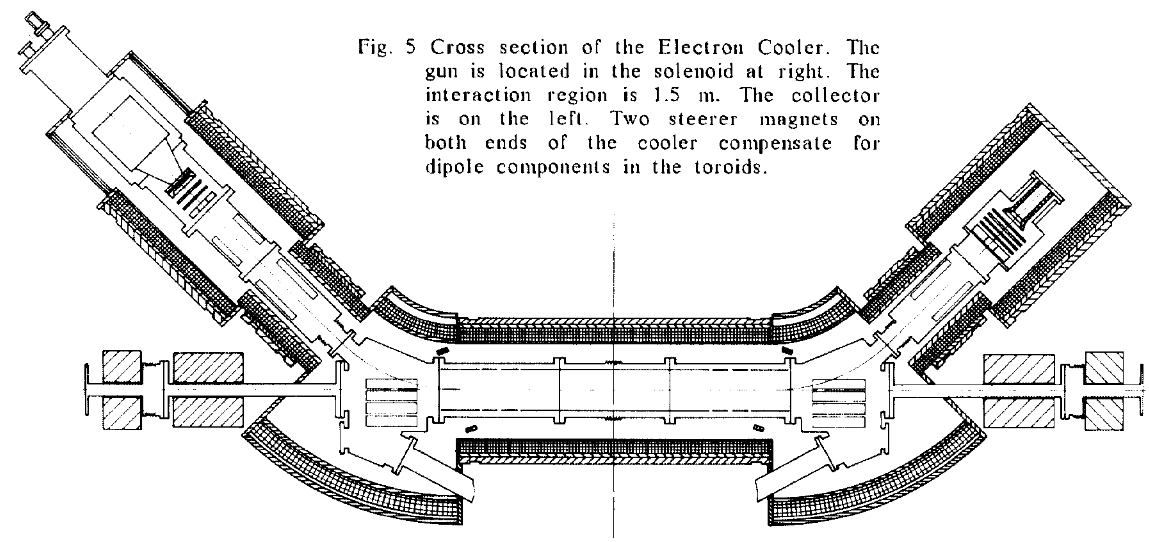

Fig. 5 Cross section of the Electron Cooler. The gun is located in the solenoid at right. The interaction region is 1.5 m. The collector is on the left. Two steerer magnets on both ends of the cooler compensate for dipole components in the toroids.

The first heavy ion beam ever cooled was C^{6+} at 6.1 MeV/amu. Almost immediately after aligning the electron beam parallel to the ion beam cooling was observed. Fig. 6 shows the evolution of a bunched beam during cooling. The time between the different traces was 150 ms. The broad bunches (lower trace) are squeezed into sharp peaks of 20 ns halfwidth. The time constant for longitudinal cooling $\tau_{1/e}$ = 240 ms.

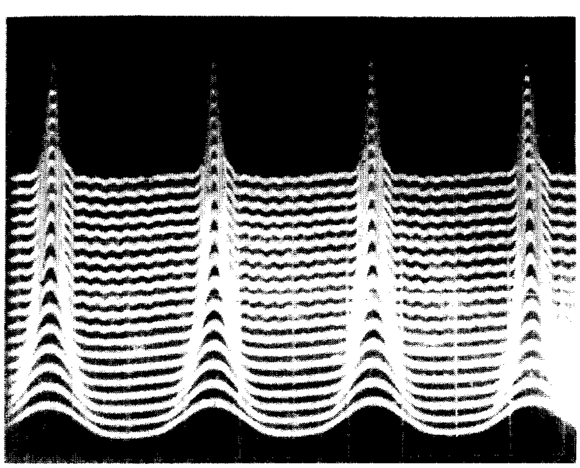

Fig. 6 Evolution of bunches during cooling. The separation of traces is 150 ms, the min. puls width is 20 ns.

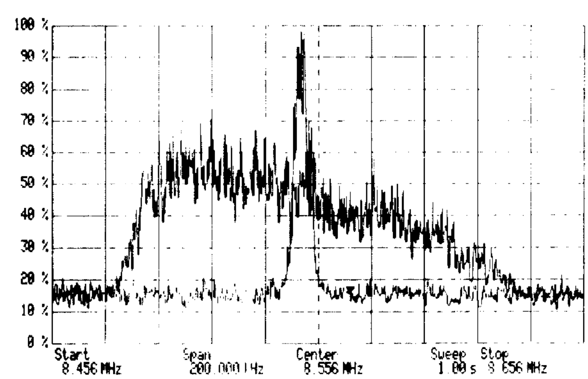

Fig. 7 Schottky noise spectrum of a rf stacked C-beam before and after cooling. The initial momentum distribution is reduced from $\Delta p/p = 2\times10^{-2}$ to $\Delta p/p = 2\times10^{-4}$.

Horizontal beam profiles where measured by scraping the beam giving reduction in beam radius by factors of up to 10 depending on the initial beam conditions. Thus the horizontal emittance had been reduced by two orders of magnitude.

Systematic investigations of longitudinal cooling gave increasing friction forces for decreasing relative velocities of ions and electrons as expected. Maximum friction force F= 1.5 eV/m was found at a relative velocity of $v = 6\times10^4$ m/s which reflects effective electron temperatures as low as T = 0.01 eV.

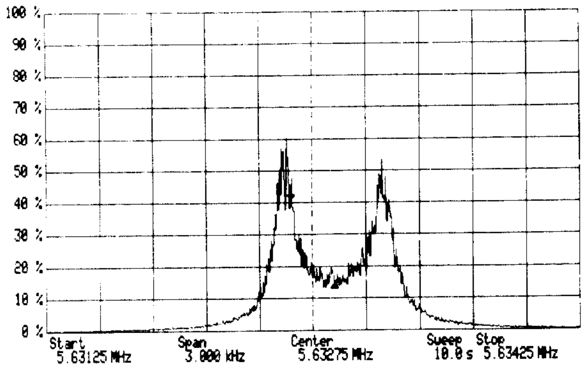

Fig. 8 Splitting of the Schottky noise spectrum for cooled intense beams.

Beam lifetime changes for cooled beam as the phase space blow up due to intrabeam scattering and multiple scattering with the residual gas is counteracted by the cooler. As for bare ions electron capture is an important loss mechanism changing the particles rigidity, beam lifetime increase has to be compared to the limits set by capture. Incompletly stripped ions as C^{5+} will experience stripping as the most dominant loss. As the vacuum conditions in the still unbaked vacuum chambers of TSR yields a mean pressure of just a few times 10^{-10} mbar, beam lifetime is limited by losses due to charge changing. Table 1 gives a summary of all beams which have been injected into TSR, some of them being cooled. The quoted mean vacuum pressure is the mean value of the gauge readings. As the residual gas composition is measured at two locations only the theoretical life time for capture and stripping, calculated from Schlachters semiempercical expression [8] and in Born approximation [9] differ necessarily up to a factor of 2 due to the bad knowledge of the heavy contaminents of the rest gas which dominate the losses especially for capture as the cross sections scale as $Z^{4.2}$.

For bare projectiles as O^{8+}, C^{6+} and proton beams electron cooling gives an increase in beam lifetime to about the limits of capture. Especially for the cooled 21 MeV proton beam the lifetime increased by a factor of 13 to 38 h. For particles which undergo stripping the present vacuum conditions prevent a more pronounced improvement in life time. On the other hand beam losses due to eletron capture in the cooler are not significant at the present conditions. This situation may substancially change when the vacuum is improved to values below 10^{-11} mbar as planned. Further studies are in preparation.

A comparison of the cooling data with previous experiments is shown in fig. 9. The plot gives the equilibrium momentum spread versus beam intensity for proton beams (labeled 'p') as have been published by the ICE experiment at CERN, the cooler at the LEAR machine, the Novosibirsk NAP-M data and the present measurements. The data fit

Table 1: Summary of beams injected and cooled at TSR. Listed are the different beams, their energies, the mean vacuum pressure, the beam lifetime measured and the theoretical limits set by multiple scattering, stripping and electron capture.

Ion	Charge state	Energy	Average pressure	Lifetime not cooled	Lifetime cooled	Theoretical Lifetime Multiple scattering	Theoretical Lifetime Capture	Theoretical Lifetime Stripping
		(MeV/a)	(10^{-11} mbar)	(s)	(s)	(s)	(s)	(s)
p	1+	21.0	8	11000	130000	8400		
Li	1+	1.3	70	1.5	1.5	188	630	5.0
C	3+	2.1	20	3.1		431	80	3.0
	4+	3.7	20	9.6		575	417	10.3
	5+	4.3	40	10.0	11.2	228	349	14.5
	6+	6.1	50	155	720	219	976	
O	3+	1.2	70	0.6		92	4	0.6
	3+	1.4	70	1.6		127	57	0.9
	3+	1.8	70	1.5		171	57	1.2
	3+	2.1	70	1.5		219	57	1.0
	3+	2.3	70	1.3		249	57	1.5
	3+	4.6	70	1.6		722	2616	2.1
	5+	2.4	20	4.5		343	55	9.0
	6+	3.4	20	14.6	15.9	412	155	19.0
	7+	4.7	50	29	34.4	192	149	24.3
	8+	6.1	50	196	258	219	318	

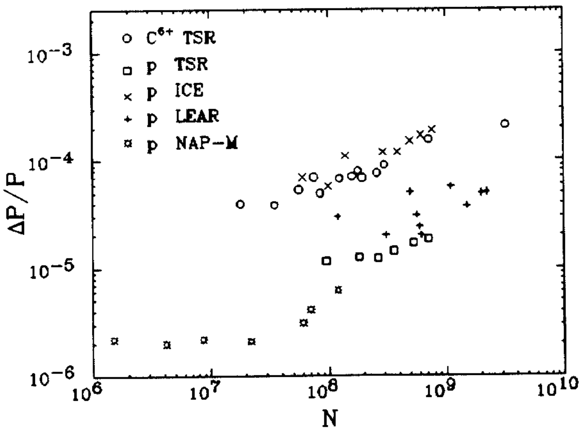

Fig. 9 Comparison of equilibrium momentum spread achieved for proton beams at CERN, Novosibirsk and present data.

exellent in between the low intensity NAP-M and the recent results at high intensities at LEAR [10]. The minimum momentum spread for $^{12}C^{6+}$ (open circles) are about a factor of Z larger due to the higher charge to mass ratio.

Acknowledgement

We would like to acknowledge the advice and help of many collegues from CERN, DESY, GSI, INS and IUCF whom we cannot name all individually. We also would like to thank the technicans of MPI for their enthusiastic and skill-full work which made the successful commissioning of TSR possible.

References

[1] G.I. Budker, N.S. Dikansky, V. I. Kudelainen, I.N. Meshkov, V.V. Parchomhuk, D.V. Pestrikov, A.N. Skrinsky, B.N. Sukhina, Particle Accelerators 7 (1976) 197.

[2] M. Bell, J. Chaney, H. Herr, F. Krienen, P. Møller-Petersen and G. Petrucci, Nucl. Instr. and Meth. 190 (1981) 235.

[3] R. Foster, T. Hardek, D.E. Johnson, W. Kells, V. Kerner, H. Lai, A.J. Lennox, F. Mills, Y. Miyahara, L. Oleksiuk, R. Peters, T. Rhodes, D. Young, P.M. McIntyre, IEEE Trans. Nucl. Sci. NS-28 (1981) 2386.

[4] E. Jaeschke, D. Krämer, W. Arnold, G. Bisoffi, M. Blum, A. Friedrich, C. Geyer, M. Grieser, D. Habs, H.W. Heyng, B. Holzer, R. Ihde, M. Jung, K. Matl, R. Neumann, A. Noda, W. Ott, B. Povh, R. Repnow, F. Schmitt, M. Steck, E. Steffens, Proc. of the 1th European Part. Acc. Conf., Rome 1988.

[5] S. Chattopadhaya, CERN 84-11.

[6] B. Huck, H. Ingwersen, E. Jaeschke, B. Kolb, R. Repnow, Th. Walcher, IEEE Trans. Nucl. Sci. NS-28 (1981) 3516.

[7] P. Thieberger, Nucl. Instr. and Meth. 220 (1984) 45.

[8] A.S. Schlachter , J.W. Stears, W.G. Graham, K.H. Berkner, R.V. Pyle and J.A. Tanis, Phys. Rev. A 27 (1983) 3372.

[9] N. Bohr, K. Dan. Vidensk. Selsk. Mat. Fys. Medd. 18 (1948) No. 8.

[10] H. Poth, W. Schwab, B. Seligmann, M. Wörtge, A. Wolf, S. Baird, M. Chanel, H. Haseroth, C.E. Hill, R. Ley, D. Manglunki, G. Tranquille, J.L. Vallet and P.F. Dittner, Z. Phys. A 332 (1989) 171.